

# Logistic-Normal Likelihoods for Heteroscedastic Label Noise in Classification

Erik Englesson<sup>1</sup> Amir Mehrpanah<sup>1</sup> Hossein Azizpour<sup>1</sup>

## Abstract

A natural way of estimating heteroscedastic label noise in regression is to model the observed (potentially noisy) target as a sample from a normal distribution, whose parameters can be learned by minimizing the negative log-likelihood. This loss has desirable loss attenuation properties, as it can reduce the contribution of high-error examples. Intuitively, this behavior can improve robustness against label noise by reducing overfitting. We propose an extension of this simple and probabilistic approach to classification that has the same desirable loss attenuation properties. We evaluate the effectiveness of the method by measuring its robustness against label noise in classification. We perform enlightening experiments exploring the inner workings of the method, including sensitivity to hyperparameters, ablation studies, and more.

## 1. Introduction

Supervised learning relies on datasets with input-label pairs, in which some labels are likely to be wrong. For classification, this could be due to annotation mistakes or measurement devices' precision in case of a regression problem.

**Heteroscedastic Noise in Regression: A Motivation.** A natural way to deal with mislabeled examples in regression is to model the observed target ( $y$ ) as the true target ( $\mu$ ) with additive noise ( $\epsilon$ ) (Nix & Weigend, 1994; Kendall & Gal, 2017; Lakshminarayanan et al., 2017):

$$y(\mathbf{x}) = \mu(\mathbf{x}) + \epsilon(\mathbf{x}) \quad (1)$$

Assuming a normally-distributed  $\epsilon$  with zero mean and variance  $\sigma^2$ , the *likelihood* of the observed target becomes  $p(y|\mathbf{x}, \mu, \sigma^2) = \mathcal{N}(y; \mu(\mathbf{x}), \sigma^2(\mathbf{x}))$ . Then, neural networks can be used to estimate the input-dependent parameters of the distribution:  $\mu(\mathbf{x}) \approx \mu_\theta(\mathbf{x})$ ,  $\sigma^2(\mathbf{x}) \approx \sigma_\theta^2(\mathbf{x})$ .

<sup>1</sup>Division of Robotics, Perception and Learning, KTH, Stockholm, Sweden. Correspondence to: Erik Englesson <engless@kth.se>.

The learning of the neural network's parameters,  $\theta$ , is typically done through some type of maximum log-likelihood estimation with  $N$  data samples:

$$\arg \max_{\theta} - \sum_{i=1}^N \frac{(y_i - \mu_\theta(\mathbf{x}_i))^2}{2\sigma_\theta^2(\mathbf{x}_i)} + \frac{1}{2} \log \sigma_\theta^2(\mathbf{x}_i) + \text{const} \quad (2)$$

This loss is of an interesting form: a label-dependent loss (mean square error) divided by the noise variance  $\sigma^2$  and a regularizing term for  $\sigma^2$  (log-partition). Hence,  $\sigma^2$  acts as an inverse importance weight of the mean square error loss. For example, for high-residual examples, the penalty of the mean-square error loss can be reduced by increasing  $\sigma^2$ , leading to higher freedom for  $\mu_\theta$  to deviate from  $y$ .

We, therefore, aim to obtain an analogously simple loss function to attenuate erroneous labels for *classification* tasks.

**Heteroscedastic Noise in Classification.** (Kendall & Gal, 2017) argued such a loss attenuation property is desirable for classification, and proposed to learn the mean and covariance of a normal distribution over the pre-softmax logits by maximizing a categorical likelihood. This results in loss attenuation, but not the same as in regression.

**Contributions.** The main contributions of our work are:

- We propose a natural extension of the above regression noise model to classification and show it leads to the observed target following a Logistic-Normal distribution (Atchison & Shen, 1980); see Section 2.2.
- We propose to use the Logistic-Normal likelihood in a maximum a posteriori estimation setting and show its negative log-likelihood has the same desirable loss attenuation properties as it can, *e.g.*, reduce the contribution of high-residual examples; see Sections 2.3 & 2.4.
- We propose important techniques and offer informative discussions for the parametrization form and formulation of the noise model parameters; see Section 3.
- We empirically study the proposed loss on synthetic datasets, synthetic noise (MNIST, CIFAR-10, CIFAR-100), and natural noise (CIFAR-N, Clothing1M) where we consistently show a significantly-improved robustness to input-dependent label noise compared to other related recent works; see Section 5.

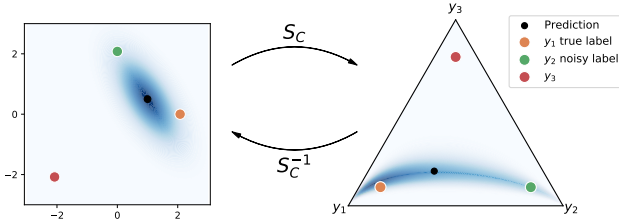


Figure 1: **Logit Space and Probability Simplex Equivalence.** Example showing how a normal distribution in  $\mathbb{R}^2$  corresponds to a Logistic-Normal distribution in  $\Delta^2$ , when using the softmax centered function as the transformation.

## 2. Method

Here, we give a high-level overview of the problem and our approach with the important details left to Section 3.

### 2.1. Background and Problem

Let us first see what we mean by class label noise, its source and why deep learning with label noise can be challenging.

**Dataset Generation.** In classification, we consider a dataset as samples of a joint distribution:  $\mathcal{D} = \{\mathbf{x}_i, y_i\}_{i=1}^N$ ,  $(\mathbf{x}_i, y_i) \sim p(\mathbf{x}, y) = p(y|\mathbf{x})p(\mathbf{x})$ . The generation process can be interpreted as first sampling the input and then the label: (i)  $\mathbf{x}_i \sim p(\mathbf{x})$ , (ii)  $y_i \sim p(y|\mathbf{x}_i)$ ; such a label  $y_i$  is thus a noisy version of the true label distribution  $p(y|\mathbf{x}_i)$ .

**Noisy Labels.** Such generation process is, in fact, how many multiclass datasets are constructed, *i.e.*, to collect a large set of inputs first and then automatically or manually annotate each input with a single output label. Hence, we approximate  $p(y|\mathbf{x}_i)$  with  $\tilde{p}(y|\mathbf{x}_i) = \delta_{y_i}$ , with  $\delta_{y_i}$  a one-hot encoding of  $y_i$ . Occasionally, sampling  $p(y|\mathbf{x})$  gives an unlikely sample  $y_i$ , *e.g.*, when errors are made in the annotation, causing a large difference between  $p(y|\mathbf{x})$  and  $\tilde{p}(y|\mathbf{x})$ . We denote this difference as label noise  $\epsilon_p(\mathbf{x}) = \tilde{p}(y|\mathbf{x}) - p(y|\mathbf{x})$  and our goal is to explicitly model  $\epsilon_p(\mathbf{x})$ .

**Learning with Label Noise.** Specifically, we are interested in a probabilistic model with parameterized output distribution  $p_\theta(y|\mathbf{x})$  and aim to optimize  $\theta$  so that  $p_\theta(y|\mathbf{x}_i) \approx p(y|\mathbf{x}_i)$  for training data  $(\mathbf{x}_i, y_i)$ . The challenge of learning from noisy labels with deep networks is their susceptibility to overfitting to  $\tilde{p}(y|\mathbf{x}_i) = \delta_{y_i}$ , for which we propose the following method and noise model.

### 2.2. Modelling Noise with Logistic-Normal Likelihoods

Inspired by the regression noise model of Equation 1, we propose to model label noise in classification via Gaussian noise in logit space (pre-softmax) and transform this distribution to the probability simplex via the softmax-centered function, resulting in a Logistic-Normal distribution. Next, we describe the noise model and likelihood in detail.

**Softmax Centered.** The softmax-centered  $S_C(z)$  is a bijective map from the logit space  $\mathbb{R}^{K-1}$  to a probability simplex for  $K$  classes  $\Delta^{K-1}$ , defined as  $S_C(z) = \text{softmax}([z_1, \dots, z_{K-1}, 0]) = [e^{z_1}, \dots, 1] / (\sum_{i=1}^{K-1} e^{z_i} + 1)$ . The bijectivity enables for a simple Gaussian noise model for the unnormalized logits, akin to the regression case.

**Noise Model.** Let us assume  $\mathbf{y}(\mathbf{x}), \boldsymbol{\mu}(\mathbf{x}), \boldsymbol{\epsilon}(\mathbf{x}) \in \mathbb{R}^{K-1}$  are vectors in the logit space,  $p(y|\mathbf{x}) = S_C(\boldsymbol{\mu}(\mathbf{x}))$  and  $\tilde{p}(y|\mathbf{x}) = S_C(\mathbf{y}(\mathbf{x}))$ . Then, applying the softmax-centered transformation to a multivariate version of Equation 1 in logit space, we get a model for label noise in classification:

$$S_C(\mathbf{y}(\mathbf{x})) = S_C(\boldsymbol{\mu}(\mathbf{x}) + \boldsymbol{\epsilon}(\mathbf{x})) \quad (3)$$

Evidently, we model the noisy target  $\tilde{p}(y|\mathbf{x})$  as the softmax-centered output of the true target logit  $\boldsymbol{\mu}$  with added Gaussian noise  $\boldsymbol{\epsilon}$ . As the map is bijective, this model gives rise to dual interpretations: (i) a Gaussian likelihood for some regression target  $\mathbf{y}(\mathbf{x})$  in the logit space, or (ii) a transformed Gaussian likelihood for a target  $S_C(\mathbf{y})$  in the probability simplex. This duality is visualized in Figure 1.

**Likelihood Function.** A zero-mean  $\boldsymbol{\epsilon}(\mathbf{x})$  with covariance  $\boldsymbol{\Sigma}(\mathbf{x})$  in Equation 3 gives the likelihood of the noisy target  $S_C(\mathbf{y}(\mathbf{x}))$  (derivation in Appendix A.1):

$$\frac{1}{\prod_{k=1}^K S_C(\mathbf{y})_k} \frac{1}{|(2\pi)^{K-1} \boldsymbol{\Sigma}|^{\frac{1}{2}}} e^{-\frac{1}{2}(\mathbf{y} - \boldsymbol{\mu})^T \boldsymbol{\Sigma}^{-1}(\mathbf{y} - \boldsymbol{\mu})} \quad (4)$$

Importantly, this corresponds to a well-studied probability density function called *Logistic-Normal distribution* (Atchison & Shen, 1980), which is a distribution over categorical distributions. In regression, the target is modelled as a sample (in  $\mathbb{R}$ ) coming from a Normal distribution over  $\mathbb{R}$ . Similarly, in classification, our method models the target as a sample (in  $\Delta^{K-1}$ ) from a Logistic-Normal distribution over  $\Delta^{K-1}$ . Note, hereafter we occasionally drop dependence of variables  $\mathbf{y}, \boldsymbol{\mu}, \boldsymbol{\Sigma}$  to  $\mathbf{x}$  for convenience.

### 2.3. Estimation with Logistic-Normal Likelihoods

We use deep networks with parameters  $\theta$  to predict the true logit vector  $\boldsymbol{\mu}_i \approx \boldsymbol{\mu}_\theta(\mathbf{x}_i)$  and the noise covariance  $\boldsymbol{\Sigma}_i \approx \boldsymbol{\Sigma}_\theta(\mathbf{x}_i)$ , per example  $i$ . We use separate linear layers for  $\boldsymbol{\mu}$  and  $\boldsymbol{\Sigma}$  that share the same backbone. The network parameters are found by minimizing the following negative log-likelihood of the dataset in addition to the negative log-prior over  $\theta$ :

$$\frac{1}{2} \sum_{i=1}^N (\mathbf{y}_i - \boldsymbol{\mu}_i)^T \boldsymbol{\Sigma}_i^{-1} (\mathbf{y}_i - \boldsymbol{\mu}_i) + \log |\boldsymbol{\Sigma}_i| + \text{const} \quad (5)$$

Note that the first factor in Equation 4 is independent of  $\theta$  and is, thus, a part of the constant term. Our goal was to find a loss function with similar loss attenuation

to the loss for regression. Comparing Equations 2 and 5, we see that our loss is almost identical to a multivariate version of the regression loss. Hence, the loss has the same attenuation effect: it can be decreased by learning  $\Sigma_i$  such that  $(\mathbf{y}_i - \boldsymbol{\mu}_i)^T \Sigma_i^{-1} (\mathbf{y}_i - \boldsymbol{\mu}_i)$  is smaller than  $(\mathbf{y}_i - \boldsymbol{\mu}_i)^T (\mathbf{y}_i - \boldsymbol{\mu}_i)$ , leading to higher freedom for  $\boldsymbol{\mu}_i$  to deviate from  $\mathbf{y}_i$  as the penalty is reduced.

We now established the *capability* for Logistic-Normal likelihood to attenuate high-residual samples and potentially predict their correct mean. Next, we do a gradient analysis whereby we show how such behavior is in fact *encouraged* when learning with gradient-following methods. In Section 5 we empirically verify the *realization* of such effect not only through the final performance on noisy training data but also with targetted analyses of the training behavior.

#### 2.4. Loss Attenuation: A Gradient Perspective

Let  $\mathcal{L}$  be the negative log-likelihood of LN distributions in Equation 5, then the gradients w.r.t.  $\boldsymbol{\mu}_j$  of example  $j$  are:

$$\frac{\partial \mathcal{L}}{\partial \boldsymbol{\mu}_j} = -\Sigma_j^{-1} (\mathbf{y}_j - \boldsymbol{\mu}_j) \quad (6)$$

This reveals an interesting form where the gradients are related to the difference between the target logit ( $\mathbf{y}_j$ ) and the predicted mean ( $\boldsymbol{\mu}_j$ ), and this difference is scaled by  $\Sigma^{-1}$ . This scaling is a major difference compared to the gradients of the negative log-likelihood of a categorical distribution (CE) w.r.t. its logits:  $-(\delta_{y_j} - S(\mathbf{z}_j))$ , where  $\mathbf{z}_j$  is the logits and  $S(\cdot)$  is the standard softmax function.

To better understand what per-example  $\Sigma$  matrices the network tries to predict, we look at the optimal covariance matrix, *i.e.*, when  $\frac{\partial \mathcal{L}}{\partial \Sigma_j} = 0$  (details in Appendix A.2):

$$\Sigma_j^{opt} = (\mathbf{y}_j - \boldsymbol{\mu}_j)(\mathbf{y}_j - \boldsymbol{\mu}_j)^T \quad (7)$$

The geometric interpretation is that the optimal density is a thin hyperellipsoid with its center on  $\boldsymbol{\mu}$  and highest variance in the direction of the noisy target  $\mathbf{y}$ , see Figure 1 left.

Using the optimal covariance matrix from Equation 7 in Equation 6, we get (details in Appendix A.3):

$$\left. \frac{\partial \mathcal{L}}{\partial \boldsymbol{\mu}_j} \right|_{\Sigma_j^{opt}} = -\frac{(\mathbf{y}_j - \boldsymbol{\mu}_j)}{\|(\mathbf{y}_j - \boldsymbol{\mu}_j)\|_2^2} \quad (8)$$

That is, for a given  $\boldsymbol{\mu}_j$ , the optimal corresponding covariance matrix divides the difference between the label and the logits by its squared l2-norm. This is exactly the loss attenuation property of the method. Clearly, the role of  $\Sigma(\mathbf{x})$  is to increase and decrease the gradients for low- and high-residual examples, respectively.

As gradients are not affected by constants, and as the LN and multivariate normal likelihoods are the same up to constants,

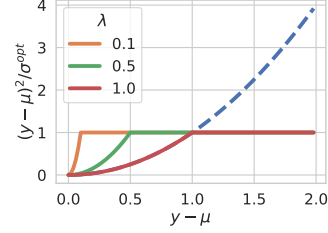


Figure 2: **Controlling Loss Attenuation with  $\lambda$ .** We plot the loss with the optimal obtainable  $\sigma^2$  (binary classification) against varying residuals. We have loss attenuation when the squared residual is larger than  $\lambda^2$ , resulting in a loss of one, and otherwise, a (scaled) squared error loss.

the gradients here also applies to the regression case. This reflects the analogy of LN for classification with the loss-attenuating regression case that we were after in this work.

### 3. Important Details

While the essence of our proposed noise model and the induced likelihood function are simple at the high level, it involves important details that we discuss in this section.

#### 3.1. Estimating Per-Example Covariance Matrices

Note that the output covariance matrix  $\Sigma(\mathbf{x})$  has  $\mathcal{O}(K^2)$  parameters, needs to be symmetric and semi-positive definite. Next, we make a structured reparametrization with  $\mathcal{O}(K)$  parameters based on the form of the optimal  $\Sigma(\mathbf{x})$ .

**Parametrization of  $\Sigma$ .** Hinging on the rank deficiency of the optimal covariance matrix, we parametrize it as  $\Sigma_{\theta}(\mathbf{x}) = \Sigma_{\theta}^{\frac{1}{2}}(\mathbf{x}) \Sigma_{\theta}^{\frac{1}{2}}(\mathbf{x})^T$  where

$$\Sigma_{\theta}^{\frac{1}{2}}(\mathbf{x}) = \mathbf{c}_{\theta}(\mathbf{x}) \mathbf{c}_{\theta}(\mathbf{x})^T + \lambda \mathbf{I}, \quad (9)$$

with  $\mathbf{c}_{\theta}(\mathbf{x}) \in \mathbb{R}^{K-1}$ , and where the hyperparameter  $\lambda \in \mathbb{R}_{>0}$ . Note that such decomposition reduces the parametrization to a rank-1 matrix,  $\mathbf{c}_{\theta}(\mathbf{x}) \mathbf{c}_{\theta}(\mathbf{x})^T$  and a positive scalar,  $\lambda$ . Therefore, it gains computational efficiency by acknowledging the singular structure of  $\Sigma^{opt}$  while crucially remaining full rank for numerical stability<sup>1</sup>.

**$\lambda$  and Loss Attenuation.** Interestingly,  $\lambda$  affects the loss beyond stability. For simplicity, consider binary classification. Then, Equation 8 becomes  $\frac{\partial \mathcal{L}}{\partial \boldsymbol{\mu}} = -(\mathbf{y} - \boldsymbol{\mu}) / \sigma^{opt} = -(\mathbf{y} - \boldsymbol{\mu}) / \|(\mathbf{y} - \boldsymbol{\mu})\|_2^2$ , and the label-dependent (first) term in Equation 5 equals one. Importantly, however, the smallest value  $\sigma_i^{opt}$  can take is  $\lambda^2$ , due to Equation 9. Thus, the label-dependent term can only attenuate the loss when  $(\mathbf{y} - \boldsymbol{\mu})^2 > \lambda^2$  and behave as a mean squared error loss divided by  $\lambda^2$  otherwise (details in Appendix A.4). We show this loss attenuation threshold behavior in Figure 2.

<sup>1</sup>Simple and efficient implementations of normal distributions with low-rank covariance matrices can be done in, *e.g.*, the distri-

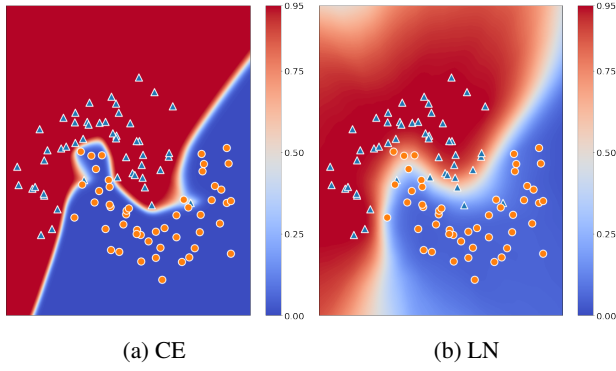


Figure 3: **Two Moons dataset.** We compare the cross entropy (a) loss with our method (b) on the Two Moons dataset, where the color corresponds to the probability of the blue triangle class. Training with CE makes the network fit all the training examples, resulting in a complex decision boundary. In contrast, the loss attenuation property of our method makes it less important to fit all examples, leading to a smooth decision boundary.

### 3.2. One-hot Targets

The noisy target  $\tilde{p}(y|x) = \delta_y$  corresponds to a corner of the probability simplex. Since softmax cannot map finite logits to the borders of the simplex, we slightly diffuse it with label smoothing:  $S_C(y) \triangleq (1-t)\delta_y + tu \in \Delta^{K-1}$ , where  $t$  is a scalar with a small fixed value, and  $\delta_y$  and  $u$  are the delta and uniform distributions over  $K$  classes, respectively.

### 3.3. The Softmax Centered Function

**Softmax-Centered with Temperature  $S_C^\tau$ .** We incorporate a temperature  $\tau$  in the softmax-centered function by seeing it as a bijective scale function:

$$S_C^\tau(z) = S_C \circ \text{Scale}_{1/\tau}(z) = S_C(z/\tau), \quad (10)$$

$$(S_C^\tau)^{-1}(p) = \text{Scale}_{1/\tau}^{-1} \circ S_C^{-1}(p) = \tau S_C^{-1}(p), \quad (11)$$

where  $z \in \mathbb{R}^{K-1}$  and  $p \in \Delta^{K-1}$ . Using the softmax centered with temperature changes the target logit in the log-likelihood of Equation 5 from  $y_i$  to  $\tau y_i = \tau S_C^{-1}((1-t)\delta_{y_i} + tu)$ . Hence, the temperature determines the magnitude of the target logit vector. We believe this has two major effects on the learning: i) a low  $\tau$  will make the target logit close to the origin and make it easy for the network to match  $\mu$  to it. A large  $\tau$  could make the learning hard as the network would have to output  $\mu$  with large magnitudes, which is penalized by the log prior (weight decay). ii) The value of  $\tau$  controls the range of residuals in the mean squared error loss. To clarify, consider a sample with a noisy target logit  $\tau y_i$ , for which the network predicts the true target  $\mu = \tau y = \tau S_C^{-1}((1-t)\delta_j + tu)$  with  $y_i \neq j$ .

buton packages of TensorFlow (Dillon et al., 2017) and PyTorch.

Then the negative log-likelihood for this example with an identity covariance is:

$$\begin{aligned} & (\tau y_i - \mu_\theta(x_i))^T (\tau y_i - \mu_\theta(x_i)) \\ &= (\tau y_i - \tau y)^T (\tau y_i - \tau y) \\ &= \tau^2 (y_i - y)^T (y_i - y) = \tau^2 C \end{aligned} \quad (12)$$

where  $C = (y_i - y)^T (y_i - y)$  is the loss without temperature scaling. Hence, the temperature determines how much the mean squared error part of the loss penalizes deviations from the observed target. We treat  $\tau$  as a hyperparameter.

**Softmax Centered with a Dummy Class.** An issue with the softmax centered function is that it treats the last class differently from the rest. To see this, we look at the target logits ( $y$ ) for target categoricals ( $S_C(y)$ ) for different classes ( $y$ ), for details see Appendix A.5. If  $y$  is not the last class, then  $y$  is zero in all components except for component  $y$  where it is a constant ( $C$ ) that depends on the number of classes  $K$ . However, if  $y$  is the last class, then all components of  $y$  are  $-C$ . See Figure 1 (left) where  $y_1 = [C, 0]$ ,  $y_2 = [0, C]$  and  $y_3 = [-C, -C]$ . This becomes a bigger problem for large  $K$ , as the squared l2-norm for an observed target logit is  $(K-1)C^2$  for the last class, and  $C^2$  otherwise.

As it is only the last class that is treated differently, we mitigate this by introducing a dummy class. We make  $S_C(y)$  be in  $\Delta^K$  by having the delta and uniform distribution be over  $K+1$  classes, and the network therefore has to output mean and covariance in  $\mathbb{R}^K$  and  $\mathbb{R}^{K \times K}$ , respectively. Then, all the  $K$  first classes that we care about are treated equally.

### 3.4. Predictions on Unseen Data

With our noise model in Equation 3, we relate the observed noisy target with the true target via an additive normally-distributed noise in the logit space. For unseen data  $x^*$ , however, we would like to predict the true target, not the noisy target, and therefore we use  $S_C(\mu_\theta(x^*))$  instead, i.e., setting  $\epsilon(x^*) = 0$ . This means that we can discard the network’s head predicting  $\Sigma$  after training.

## 4. Related Work

**Heteroscedastic Noise Estimation.** Nix & Weigend (1994) tackle the problem of input-dependent noise, for regression, in a maximum likelihood estimation framework. They assume an additive Gaussian label noise and optimize two different networks to predict the mean and the variance of the output distributions. Kendall & Gal (2017) importantly, note that such a framework provides a model with the capacity to effectively attenuate the loss induced by samples which are hard to model (Equation 2) and thus renders it possibly robust to label noise. More, they argue such attenuation properties are also desirable in classification and propose



a method termed Heteroscedastic Classification NNs (Het). They place a normal distribution over the pre-softmax logits to model heteroscedastic uncertainty/noise, which is then marginalized out to obtain a categorical distribution:

$$\mathbb{E}_{\epsilon \sim \mathcal{N}(0, \Sigma_\theta(x_i))} [S(\mu_\theta(x_i) + \epsilon)] \quad (13)$$

where  $\mu \in \mathbb{R}^K$ , and  $\Sigma \in \mathbb{R}^{K \times K}$  is a diagonal covariance matrix, both predicted per-example by a neural network. The negative log-likelihood of this categorical distribution is then used as the loss *i.e.*, cross-entropy. Collier et al. (2020) extended this by tempering the softmax (Het- $\tau$ ), and evaluated the robustness of the method to label noise. In yet another work, (Collier et al., 2021) proposed an efficient way of parameterizing a full covariance matrix (Het- $\tau$ - $\Sigma_{full}$ ), which is similar to ours in Equation 9. To better understand this family of works, we analyse the gradients w.r.t.  $\mu$  for sample  $i$  with label  $y_i = c$  (derivation in Appendix A.6):

$$-\left( \delta_c - \mathbb{E}_\epsilon \left[ S(\mu_i + \epsilon) \frac{S(\mu_i + \epsilon)_c}{\mathbb{E}_\epsilon [S(\mu_i + \epsilon)_c]} \right] \right) \quad (14)$$

Comparing with the expectation in Equation 13, we see it is modified for the gradients to increase the contribution of each sampled categorical distribution  $S(\mu_i + \epsilon)$  that has a high confidence in the given class,  $S(\mu_i + \epsilon)_c$ . Clearly, this is doing loss attenuation as the network could learn to add noise to increase the confidence in the given class, making the expected categorical be closer to the target onehot distribution. However, the loss attenuation of this method is different from the one in maximum likelihood estimation with Normal (regression) and Logistic-Normal (classification) likelihoods, see Section 2.4. We empirically compare Logistic Normal with all the variants in this line of work.

**Loss Correction.** Closest to our work are the loss correction methods that estimate the true categorical distribution and transforms it to the observed noisy one (Sukhbaatar et al., 2014; Patrini et al., 2017):  $\tilde{p}(y|x) = Tp(y|x)$ , where  $T$  is a matrix with elements  $T_{ij}$  estimating the probability that the noisy class is  $j$ , given that the true class is  $i$ . This is clearly related to our noise model, as we transform the true categorical to the noisy one by adding noise in logit space. Importantly, we estimate a covariance matrix per example while these works estimate a single matrix  $T$  per dataset.

**Loss Reweighting.** These methods propose to weight the per-example losses to reduce the contribution of noisy examples. The weights can be estimated through density estimation (Liu & Tao, 2015), or predicted by the same network (Wang et al., 2017; Thulasidasan et al., 2019), another network (Jiang et al., 2018), or via meta-learning (Ren et al., 2018). Typically, these reweighting mechanisms are manually-designed, making the explicit assumption on the probabilistic likelihood function unclear. Our method can be seen as a simple principled way of doing loss reweighting.

**Robust Loss Functions.** Ghosh et al. (2017) proved that, for certain (symmetric) loss functions, the globally optimal classifier is the same when trained with noise-free data as when trained with symmetric or asymmetric noise, under certain assumptions. Based on this theory, several new loss functions have been proposed (Zhang & Sabuncu, 2018; Wang et al., 2019; Ma et al., 2020; Engleson & Azizpour, 2021) and even extensions of the theory to a broader class of losses (Zhou et al., 2021). There are also many other theoretically motivated robust loss functions (Amid et al., 2019; Xu et al., 2019; Wei & Liu, 2021).

**Regularization.** Several standard regularization methods have also been studied when training with label noise, *e.g.*, label smoothing (Lukasik et al., 2020), dropout (Rusiecki, 2020; Goel & Chen, 2021), and early stopping (Li et al., 2020b; Bai et al., 2021). Furthermore, some methods regularize the predictions of the network to be consistent with the moving average of predictions from earlier in training (Liu et al., 2020; Laine & Aila, 2017), while others add noise to the gradients, *e.g.*, by adding noise to the one-hot labels (Chen et al., 2020).

## 5. Results

Now we empirically verify that our theoretically motivated method demonstrates robustness to label noise. We first describe the common training setup for all methods (Section 5.1), then comes a detailed description of the baselines (Section 5.2), followed by the results on synthetic datasets (Section 5.3), synthetic label noise (Section 5.4), and natural label noise (Section 5.5). Finally, additional studies are conducted which provides further insights on different aspects of our method (Section 5.6).

### 5.1. Experimental Setup

We implement our method and all the baselines in the same code base and compare on the following datasets: Two Moons & Circles, MNIST (Deng, 2012), CIFAR-10 & CIFAR-100 (Krizhevsky et al., 2009), CIFAR-10N & CIFAR-100N (Wei et al., 2022), and Clothing1M (Xiao et al., 2015). For all methods, and on all datasets, we search for method-specific hyperparameters based on noisy validation accuracy at the end of training. We report the mean and standard deviation of the test accuracy at the end of training for five different random seeds with the optimal hyperparameters. The seeds affect the network initialization, data loaders, and the generation of the synthetic label noise. For details about the experimental setup, see Appendix B.

### 5.2. Baselines

In addition to the standard cross-entropy (CE) loss, we compare our method with a number of works that share the same

Table 1: **Synthetic Noise on MNIST, CIFAR-10 and CIFAR-100.** We implement our method and all baselines in the same shared code based and do a search for the best hyperparameters on a noisy validation set for all methods. We report the mean and standard deviation of the test accuracy from five runs with different random seeds. Results in bold correspond to the methods with no statistically significant difference to the method with the highest mean. Our method (LN) shows strong performance compared to baselines, especially on the predictable asymmetric noise, and the challenging CIFAR-100 dataset.

Method	No Noise	Symmetric Noise Rate					Asymmetric Noise Rate			
	0%	20%	40%	60%	80%		10%	20%	30%	40%
MNIST	CE	99.27 $\pm$ 0.07	88.41 $\pm$ 0.34	70.67 $\pm$ 1.30	51.04 $\pm$ 1.19	29.53 $\pm$ 1.08	96.64 $\pm$ 0.32	91.09 $\pm$ 0.79	86.31 $\pm$ 1.25	80.31 $\pm$ 1.81
	Bi-tempered	99.22 $\pm$ 0.05	97.79 $\pm$ 0.69	97.78 $\pm$ 0.29	83.26 $\pm$ 1.50	53.76 $\pm$ 2.58	96.52 $\pm$ 0.28	97.33 $\pm$ 0.16	96.67 $\pm$ 0.51	86.45 $\pm$ 1.79
	GCE	99.22 $\pm$ 0.06	<b>98.85 <math>\pm</math> 0.18</b>	<b>98.60 <math>\pm</math> 0.11</b>	<b>97.45 <math>\pm</math> 0.31</b>	<b>92.60 <math>\pm</math> 0.61</b>	98.98 $\pm$ 0.12	98.52 $\pm$ 0.31	86.36 $\pm$ 0.86	79.81 $\pm$ 1.46
	NAN	98.44 $\pm$ 0.24	97.51 $\pm$ 0.37	90.03 $\pm$ 0.95	74.00 $\pm$ 2.92	46.25 $\pm$ 2.03	97.04 $\pm$ 1.23	96.46 $\pm$ 2.23	95.43 $\pm$ 1.09	88.95 $\pm$ 1.63
	Forward	99.27 $\pm$ 0.03	87.46 $\pm$ 0.70	69.96 $\pm$ 2.10	50.43 $\pm$ 1.43	30.01 $\pm$ 0.60	96.51 $\pm$ 0.55	91.95 $\pm$ 0.40	86.31 $\pm$ 0.43	80.97 $\pm$ 1.23
	Het	99.28 $\pm$ 0.05	87.09 $\pm$ 0.70	70.30 $\pm$ 1.10	50.57 $\pm$ 1.02	29.88 $\pm$ 0.88	96.45 $\pm$ 0.35	91.12 $\pm$ 1.29	86.35 $\pm$ 0.62	80.04 $\pm$ 0.87
	Het- $\tau$	99.25 $\pm$ 0.07	88.10 $\pm$ 0.70	70.19 $\pm$ 1.58	51.95 $\pm$ 1.13	31.81 $\pm$ 0.86	96.07 $\pm$ 0.45	91.13 $\pm$ 1.25	85.95 $\pm$ 0.69	81.37 $\pm$ 1.14
	Het- $\tau$ - $\Sigma_{full}$	<b>99.25 <math>\pm</math> 0.15</b>	89.16 $\pm$ 0.44	70.34 $\pm$ 1.20	50.89 $\pm$ 1.79	30.54 $\pm$ 0.69	96.74 $\pm$ 0.19	91.06 $\pm$ 0.24	86.25 $\pm$ 0.88	79.93 $\pm$ 0.44
	LN	<b>99.38 <math>\pm</math> 0.06</b>	<b>98.53 <math>\pm</math> 0.27</b>	97.21 $\pm$ 0.38	90.93 $\pm$ 2.29	60.15 $\pm$ 5.01	<b>99.24 <math>\pm</math> 0.06</b>	<b>99.19 <math>\pm</math> 0.10</b>	<b>99.01 <math>\pm</math> 0.19</b>	<b>96.54 <math>\pm</math> 1.20</b>
CIFAR-10	CE	<b>90.67 <math>\pm</math> 0.80</b>	73.54 $\pm$ 1.01	56.56 $\pm$ 1.44	39.44 $\pm$ 1.87	21.91 $\pm$ 1.35	85.56 $\pm$ 0.53	81.35 $\pm$ 1.26	76.01 $\pm$ 2.67	71.89 $\pm$ 1.67
	Bi-tempered	89.89 $\pm$ 0.50	85.68 $\pm$ 0.38	75.70 $\pm$ 2.16	51.55 $\pm$ 4.66	32.18 $\pm$ 2.31	85.49 $\pm$ 0.75	81.79 $\pm$ 1.40	78.74 $\pm$ 1.66	71.60 $\pm$ 1.37
	GCE	<b>90.83 <math>\pm</math> 0.44</b>	<b>87.55 <math>\pm</math> 0.41</b>	<b>84.72 <math>\pm</math> 0.82</b>	<b>79.25 <math>\pm</math> 0.93</b>	<b>64.28 <math>\pm</math> 1.42</b>	<b>88.02 <math>\pm</math> 0.20</b>	85.68 $\pm$ 0.69	83.97 $\pm$ 0.52	72.90 $\pm$ 1.61
	NAN	89.61 $\pm$ 0.93	83.86 $\pm$ 1.03	79.80 $\pm$ 0.59	73.58 $\pm$ 0.41	61.06 $\pm$ 1.84	86.55 $\pm$ 0.72	84.32 $\pm$ 1.05	76.79 $\pm$ 2.28	72.90 $\pm$ 1.92
	Forward	<b>90.69 <math>\pm</math> 0.38</b>	74.39 $\pm$ 1.49	59.60 $\pm$ 1.40	40.06 $\pm$ 2.16	23.80 $\pm$ 1.00	86.17 $\pm$ 0.65	82.10 $\pm$ 1.09	77.02 $\pm$ 2.38	72.77 $\pm$ 1.43
	Het	<b>90.41 <math>\pm</math> 0.69</b>	74.67 $\pm$ 1.06	58.53 $\pm$ 1.96	39.51 $\pm$ 2.53	24.18 $\pm$ 0.67	86.26 $\pm$ 0.40	81.72 $\pm$ 1.65	76.97 $\pm$ 1.17	72.88 $\pm$ 1.53
	Het- $\tau$	<b>91.18 <math>\pm</math> 0.41</b>	76.90 $\pm$ 1.79	63.55 $\pm$ 2.27	44.73 $\pm$ 1.67	26.36 $\pm$ 1.58	86.02 $\pm$ 0.61	81.40 $\pm$ 0.96	77.41 $\pm$ 2.53	72.53 $\pm$ 1.83
	Het- $\tau$ - $\Sigma_{full}$	<b>90.82 <math>\pm</math> 0.42</b>	77.16 $\pm$ 0.94	62.85 $\pm$ 1.88	44.20 $\pm$ 3.05	25.11 $\pm$ 2.20	86.41 $\pm$ 0.55	81.55 $\pm$ 0.80	77.05 $\pm$ 0.33	72.69 $\pm$ 0.89
	LN	90.17 $\pm$ 0.55	86.13 $\pm$ 1.03	81.37 $\pm$ 1.97	76.08 $\pm$ 0.63	<b>63.58 <math>\pm</math> 1.76</b>	<b>88.25 <math>\pm</math> 0.53</b>	<b>87.64 <math>\pm</math> 0.78</b>	<b>86.91 <math>\pm</math> 1.03</b>	<b>82.18 <math>\pm</math> 1.30</b>
CIFAR-100	CE	<b>64.87 <math>\pm</math> 0.88</b>	47.39 $\pm$ 0.43	33.62 $\pm$ 0.79	20.04 $\pm$ 0.58	7.38 $\pm$ 0.12	57.52 $\pm$ 0.65	50.98 $\pm$ 0.88	44.04 $\pm$ 0.73	36.95 $\pm$ 0.58
	Bi-tempered	<b>64.75 <math>\pm</math> 0.15</b>	58.32 $\pm$ 0.69	49.05 $\pm$ 0.47	29.51 $\pm$ 0.67	10.53 $\pm$ 0.67	60.17 $\pm$ 0.79	53.04 $\pm$ 0.94	44.96 $\pm$ 0.52	36.95 $\pm$ 0.90
	GCE	<b>64.33 <math>\pm</math> 0.83</b>	<b>61.67 <math>\pm</math> 0.67</b>	<b>53.96 <math>\pm</math> 1.40</b>	42.85 $\pm$ 0.79	10.77 $\pm$ 0.28	<b>62.34 <math>\pm</math> 0.67</b>	59.63 $\pm$ 1.28	49.21 $\pm$ 0.53	36.78 $\pm$ 0.50
	NAN	<b>64.25 <math>\pm</math> 0.64</b>	56.93 $\pm$ 0.77	50.03 $\pm$ 0.62	40.45 $\pm$ 0.41	<b>24.00 <math>\pm</math> 0.59</b>	60.55 $\pm$ 0.71	56.40 $\pm$ 1.07	52.78 $\pm$ 0.85	40.59 $\pm$ 0.84
	Forward	<b>64.33 <math>\pm</math> 0.73</b>	47.90 $\pm$ 0.93	32.28 $\pm$ 1.10	20.00 $\pm$ 0.75	7.64 $\pm$ 0.28	58.46 $\pm$ 0.53	50.82 $\pm$ 0.57	43.87 $\pm$ 0.47	37.02 $\pm$ 0.72
	Het	<b>64.48 <math>\pm</math> 0.31</b>	48.40 $\pm$ 1.32	34.26 $\pm$ 0.37	20.33 $\pm$ 0.31	7.66 $\pm$ 0.38	58.18 $\pm$ 0.31	51.44 $\pm$ 1.15	45.09 $\pm$ 0.40	37.43 $\pm$ 0.66
	Het- $\tau$	<b>64.20 <math>\pm</math> 0.37</b>	54.17 $\pm$ 0.79	42.03 $\pm$ 0.84	22.33 $\pm$ 0.57	7.31 $\pm$ 0.37	<b>62.71 <math>\pm</math> 0.75</b>	59.89 $\pm$ 0.54	53.75 $\pm$ 1.08	41.14 $\pm$ 0.98
	Het- $\tau$ - $\Sigma_{full}$	<b>65.18 <math>\pm</math> 0.90</b>	54.83 $\pm$ 0.46	41.49 $\pm$ 1.53	22.42 $\pm$ 0.95	7.77 $\pm$ 0.27	61.88 $\pm$ 0.85	61.29 $\pm$ 0.46	56.44 $\pm$ 0.53	45.75 $\pm$ 1.02
	LN	<b>64.88 <math>\pm</math> 0.98</b>	<b>60.58 <math>\pm</math> 1.07</b>	<b>55.55 <math>\pm</math> 1.30</b>	<b>46.43 <math>\pm</math> 1.15</b>	<b>23.64 <math>\pm</math> 1.02</b>	<b>63.35 <math>\pm</math> 0.75</b>	<b>64.31 <math>\pm</math> 0.98</b>	<b>64.07 <math>\pm</math> 0.77</b>	<b>61.20 <math>\pm</math> 1.22</b>

Table 2: **Natural Noise: CIFAR-10N, CIFAR-100N, and Clothing1M.** For all methods, we search for method-specific hyperparameters based on a noisy validation set and report the mean and standard deviation for the best setting. Our method performs as well as other baselines or is a close second to the robust GCE (Zhang & Sabuncu, 2018) loss.

Method	CIFAR-10N					CIFAR-100N	Clothing1M
	Random 1	Random 2	Random 3	Aggregate	Worst		
CE	77.75 $\pm$ 0.74	75.52 $\pm$ 1.08	76.25 $\pm$ 1.26	83.59 $\pm$ 0.98	59.01 $\pm$ 0.98	42.75 $\pm$ 0.93	71.04 $\pm$ 0.15
Bi-tempered	83.65 $\pm$ 1.43	83.31 $\pm$ 1.41	82.67 $\pm$ 0.83	<b>86.17 <math>\pm</math> 0.73</b>	69.83 $\pm$ 1.36	47.94 $\pm$ 1.13	71.92 $\pm$ 0.14
GCE	<b>85.66 <math>\pm</math> 0.73</b>	<b>85.58 <math>\pm</math> 0.65</b>	<b>84.78 <math>\pm</math> 0.62</b>	<b>86.66 <math>\pm</math> 0.68</b>	<b>77.48 <math>\pm</math> 1.22</b>	48.81 $\pm$ 0.46	71.95 $\pm$ 0.21
NAN	81.85 $\pm$ 1.13	83.40 $\pm$ 0.84	82.77 $\pm$ 0.78	85.53 $\pm$ 0.83	75.47 $\pm$ 0.76	<b>50.00 <math>\pm</math> 0.72</b>	71.50 $\pm$ 0.41
Forward	77.97 $\pm$ 0.80	77.13 $\pm$ 0.74	77.51 $\pm$ 1.21	83.58 $\pm$ 1.50	58.91 $\pm$ 0.57	42.53 $\pm$ 0.41	70.75 $\pm$ 0.25
Het	76.38 $\pm$ 0.97	75.85 $\pm$ 1.45	76.18 $\pm$ 1.60	83.87 $\pm$ 1.02	58.86 $\pm$ 1.27	42.90 $\pm$ 0.48	70.87 $\pm$ 0.38
Het- $\tau$	78.83 $\pm$ 1.65	78.29 $\pm$ 1.61	78.27 $\pm$ 0.86	84.34 $\pm$ 0.48	62.01 $\pm$ 2.03	45.82 $\pm$ 0.53	<b>72.24 <math>\pm</math> 0.30</b>
Het- $\tau$ - $\Sigma_{full}$	78.87 $\pm$ 0.47	76.24 $\pm$ 0.96	77.68 $\pm$ 1.93	84.45 $\pm$ 0.57	63.27 $\pm$ 2.62	45.58 $\pm$ 0.80	<b>72.41 <math>\pm</math> 0.15</b>
LN	83.70 $\pm$ 0.80	83.65 $\pm$ 0.82	<b>84.07 <math>\pm</math> 0.71</b>	<b>85.35 <math>\pm</math> 1.33</b>	74.31 $\pm$ 1.08	<b>50.37 <math>\pm</math> 0.50</b>	<b>72.03 <math>\pm</math> 0.52</b>

motivation and goal in having a method that deals with heteroscedastic label noise similar to the simple and efficient probabilistic method for regression: Het (Kendall & Gal, 2017), Het- $\tau$  (Collier et al., 2020), and Het- $\tau$ - $\Sigma_{full}$  (Collier et al., 2021). Common to our method and these baselines

is the modelling of the pre-softmax logit vector as being normally distributed and the use of a deep neural network to output the mean and covariance of this distribution. Another relevant work we compare with is the loss correction approach of Forward (Patrini et al., 2017). In addition to

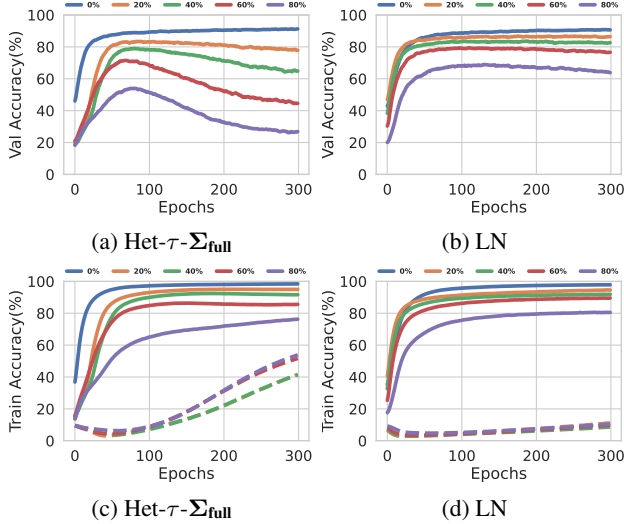


Figure 4: **The Evolution of Validation and Training Accuracy.** We plot the noise-free validation accuracy (top) and noisy training accuracy (bottom) of  $\text{Het-}\tau\text{-}\Sigma_{\text{full}}$  and our method (LN) on varying symmetric noise rates during training on CIFAR-10. We report the training accuracy of noise-free (full) and noisy (dashed) examples separately. We observe that the generalization degrades (a) for networks trained with  $\text{Het-}\tau\text{-}\Sigma_{\text{full}}$  as it fits the noisy examples (c). Our method results in better generalization (b) and is more robust against fitting the noisy examples of the training set (d).

these highly related works, for completeness, we compare with several other baselines : Generalized Cross Entropy (GCE) (Zhang & Sabuncu, 2018), Bi-tempered (Amid et al., 2019), and Noise Against Noise (NAN) (Chen et al., 2020).

### 5.3. Synthetic Dataset: Two Moons

In Figure 3, we compare the behavior of our method (LN) with the cross entropy (CE) loss on the two moons dataset. We find that training with the CE loss makes the network classify almost all examples according to their observed targets, resulting in a complex decision boundary that does not generalize well. In contrast, the network trained with the log-likelihood of the Logistic-Normal distribution has a smoother decision boundary as the network is not classifying some examples as their given targets.

### 5.4. Synthetic Noise

**Noise types.** Here, we study our method on two types of synthetic class-dependent label noise (asymmetric and symmetric). For each training sample, there is a risk (according to the noise rate) that its label is randomly re-sampled from a uniform distribution over the classes (symmetric noise) or changed to another, often perceptually similar, class (asymmetric). The asymmetric noise changes the la-

Table 3: **Ablation Study.** We analyse the effect of learning  $\Sigma$ , different parameterizations, as well as the effect of the dummy class. Learning a full  $\Sigma$  performs the best, and the dummy class is crucial for datasets with many classes.

$\Sigma$	Dummy Class	CIFAR-10N	CIFAR-100N
Identity	✓	65.64 $\pm$ 1.53	47.69 $\pm$ 1.46
Isotropic	✓	71.12 $\pm$ 1.85	46.44 $\pm$ 0.67
Diagonal	✓	69.87 $\pm$ 1.11	46.98 $\pm$ 0.89
Full	✓	<b>74.31 <math>\pm</math> 1.08</b>	<b>50.37 <math>\pm</math> 0.50</b>
Full	✗	<b>74.72 <math>\pm</math> 1.14</b>	26.31 $\pm$ 1.43

bels as follows: MNIST: 7  $\rightarrow$  1, 2  $\rightarrow$  7, 5  $\leftrightarrow$  6, 3  $\rightarrow$  8, CIFAR-10: bird  $\rightarrow$  airplane, cat  $\leftrightarrow$  dog, deer  $\rightarrow$  horse, CIFAR-100: cyclically to the next class, *e.g.*, 1  $\rightarrow$  2 and 99  $\rightarrow$  0.

**Results.** Table 1 shows the results using symmetric and asymmetric label noise. Compared to the most related works (Forward and Het methods), we find that the test accuracy of our method is degraded the least for all noise types and rates. Out of the more general set of baselines, we find that the robust GCE loss performs remarkably well on symmetric noise. Our method shows largest improvements in robustness for the more challenging CIFAR-100 dataset, as well as for asymmetric noise. For example, on CIFAR-100 with 40% asymmetric noise, our method achieves a mean test error of  $\sim 61\%$  compared to  $\sim 46\%$  of the best baseline. We find that the generalization of the networks trained with our method is barely affected when increasing asymmetric noise rates from 10% to 30% on all datasets. This is likely due to the predictable structure of the asymmetric noise, which could also explain why our method fall behind the robust GCE loss on symmetric noise, as it is inherently unpredictable and has to be memorized.

### 5.5. Natural Noise

**Datasets.** Synthetic label noise is excellent for performing experiments to understand robustness to noise under controlled noise rates. However, this comes at the cost of the structure of the noise (class-dependent) potentially being different from what one would observe in practice (input-dependent), *e.g.*, due to mistakes in the annotation process. In this section, we study the robustness of our method on natural noise by using the recently proposed CIFAR-N datasets (Wei et al., 2022) and Clothing1M (Xiao et al., 2015), see Appendix C for more information.

**Results.** Table 2 shows the test accuracy of our method on naturally noisy datasets. Compared to the most relevant baselines (Forward and Het methods), we find that networks trained with our method generalize better on the CIFAR-N datasets, and as good as  $\text{Het-}\tau$  and  $\text{Het-}\tau\text{-}\Sigma_{\text{full}}$  on Clothing1M. For the more general set of baselines, Bi-tempered, NAN and especially GCE are strong baselines in this setting.

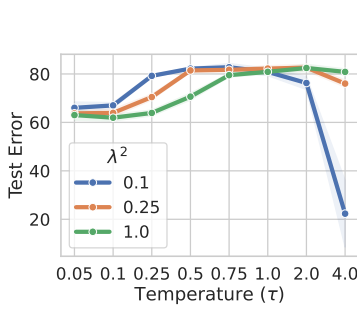


Figure 5: **Sensitivity to Hyperparameters.** The mean and standard deviation of test accuracy for various hyperparameters on CIFAR-10 with 40% symmetric noise. A too small  $\tau$  leads to overfitting to noise, while a too large  $\tau$  and  $\lambda$  leads to slow convergence.

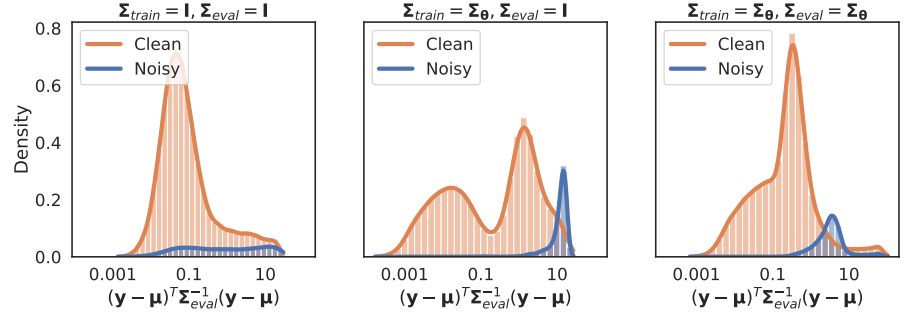


Figure 6: **Histogram of Residuals.** We train two LN networks with different covariance matrices:  $\Sigma_{train} = I$ , and  $\Sigma_{train} = \Sigma_{\theta}$ . At the end of training, we calculate the distributions of the label-dependent term of the loss,  $(y - \mu)^T \Sigma_{eval}^{-1} (y - \mu)$ , on the CIFAR-10 training set with 20% asymmetric noise. We compare  $\Sigma_{train} = \Sigma_{eval} = I$  (left), and for the network with  $\Sigma_{train} = \Sigma_{\theta}$ , we use  $\Sigma_{eval} = I$  (middle), and  $\Sigma_{eval} = \Sigma_{\theta}$  (right). We find that  $\mu$  fits less of the noisy examples when learning  $\Sigma$  (cf. left and middle), and that  $\Sigma_{\theta}$  increases and decreases the contribution of low- and high-residual examples, respectively (cf. middle and right).

## 5.6. Empirical Study of LN

**How does the accuracy evolve during training?** Figure 4 shows the clean validation and noisy training accuracy during training on CIFAR-10 with symmetric noise for various noise rates for Het- $\tau$ - $\Sigma_{full}$  and our method. We report the training accuracy for the clean and noisy subsets separately. The generalization of models trained with Het- $\tau$ - $\Sigma_{full}$  is improved early in training as the networks fit the correctly labeled examples, and when the networks start fitting the noisy examples, the generalization degrades significantly. In contrast, we find that networks trained with our method fit significantly less noisy examples and thus show a smaller decrease in generalization.

**How sensitive is LN to hyperparameters?** See Figure 5. A small  $\tau$  makes the network overfit, likely due to the target logit being close to the origin (Equation 11), thus easy to fit. A large  $\tau$  with a small  $\lambda$  leads to slow convergence, likely due to some clean examples being loss attenuated as  $\tau$  increases residuals (Equation 12), making examples more likely to be above the loss attenuation threshold, see last paragraph in Section 3.1.

**How important is learning a full  $\Sigma_{\theta}(x)$  matrix?** In Table 3, we train LN likelihoods on CIFAR-10N (noise type "worst") and CIFAR-100 with different per-example covariance matrices:  $I$  (Identity),  $\sigma^2 I$  (Isotropic),  $\text{diag}([\sigma_1^2, \dots, \sigma_K^2])$  (Diag), and the parametrization in Equation 9 (Full). First, we note that using an identity matrix generalizes significantly worse than all the other learnable ones, highlighting the importance of loss attenuation. Secondly, we find our proposed parametrization (Full) to perform significantly better than the rest.

**How important is the dummy class?** Our analysis in Sec-

tion 3.3 highlighted that the softmax centered treated the last class differently, and that this difference increased with the number of classes. In Table 3, we evaluate the importance of our solution (dummy class) to this problem. As expected, on CIFAR-10, it makes no significant difference, however, on CIFAR-100 with its many more classes, it becomes crucial.

**How is  $\Sigma_{\theta}(x)$  affecting the network?** In Figure 6, a network trained with an identity matrix has, as expected, more noisy examples with lower residuals (a), compared to the network that learns the covariance matrix (b). Interestingly, the residuals in b) are bimodal, which we believe is due to some clean examples being below the learnable loss attenuation threshold (Section 3.1) and some above. Comparing Figure 6 b) and c), we find that  $\Sigma_{\theta}$  is increasing the residuals of some clean examples, while also reducing the residuals of noisy ones mixed with some (hard) clean samples. These results are for the CIFAR-10 training set with 20% asymmetric noise, see Appendix E.1 for more noise types.

## 6. Conclusion

The goal of this work was to extend the simple and probabilistic approach of doing loss attenuation in regression to classification. We successfully achieved this by proposing a noise model that lead to the Logistic-Normal distribution. We proposed to learn the parameters of the distribution with neural networks through maximum likelihood estimation and formally presented the loss attenuation effects obtained when optimizing such models. Finally, we empirically verified that LN is effectively robust to label noise. As our method has the same loss attenuation as in the regression case, it can serve as a simple alternative to the methods of (Kendall & Gal, 2017; Collier et al., 2020; 2021).



**Acknowledgement.** This work was partially supported by the Wallenberg AI, Autonomous Systems and Software Program (WASP) funded by the Knut and Alice Wallenberg Foundation.

## References

- Amid, E., Warmuth, M. K., Anil, R., and Koren, T. Robust bi-tempered logistic loss based on bregman divergences. *Advances in Neural Information Processing Systems*, 32, 2019.
- Atchison, J. and Shen, S. M. Logistic-normal distributions: Some properties and uses. *Biometrika*, 67(2):261–272, 1980.
- Bai, Y., Yang, E., Han, B., Yang, Y., Li, J., Mao, Y., Niu, G., and Liu, T. Understanding and improving early stopping for learning with noisy labels. *Advances in Neural Information Processing Systems*, 34:24392–24403, 2021.
- Chen, P., Chen, G., Ye, J., Heng, P.-A., et al. Noise against noise: stochastic label noise helps combat inherent label noise. In *International Conference on Learning Representations*, 2020.
- Collier, M., Mustafa, B., Kokiopoulou, E., Jenatton, R., and Berent, J. A simple probabilistic method for deep classification under input-dependent label noise. *arXiv preprint arXiv:2003.06778*, 2020.
- Collier, M., Mustafa, B., Kokiopoulou, E., Jenatton, R., and Berent, J. Correlated input-dependent label noise in large-scale image classification. In *Proceedings of the IEEE/CVF Conference on Computer Vision and Pattern Recognition*, pp. 1551–1560, 2021.
- Deng, L. The mnist database of handwritten digit images for machine learning research. *IEEE Signal Processing Magazine*, 29(6):141–142, 2012.
- Dillon, J. V., Langmore, I., Tran, D., Brevdo, E., Vasudevan, S., Moore, D., Patton, B., Alemi, A., Hoffman, M. D., and Saurous, R. A. Tensorflow distributions. *CoRR*, abs/1711.10604, 2017. URL <http://arxiv.org/abs/1711.10604>.
- Engleson, E. and Azizpour, H. Generalized jensen-shannon divergence loss for learning with noisy labels. *Advances in Neural Information Processing Systems*, 34:30284–30297, 2021.
- Ghosh, A., Kumar, H., and Sastry, P. S. Robust loss functions under label noise for deep neural networks. In *Proceedings of the AAAI conference on artificial intelligence*, volume 31, 2017.
- Goel, P. and Chen, L. On the robustness of monte carlo dropout trained with noisy labels. In *Proceedings of the IEEE/CVF Conference on Computer Vision and Pattern Recognition*, pp. 2219–2228, 2021.
- Harville, D. A. Matrix algebra from a statistician’s perspective, 1998.
- Jiang, L., Zhou, Z., Leung, T., Li, L.-J., and Fei-Fei, L. Mentornet: Learning data-driven curriculum for very deep neural networks on corrupted labels. In *International conference on machine learning*, pp. 2304–2313. PMLR, 2018.
- Kendall, A. and Gal, Y. What uncertainties do we need in bayesian deep learning for computer vision? *Advances in neural information processing systems*, 30, 2017.
- Krizhevsky, A., Hinton, G., et al. Learning multiple layers of features from tiny images. 2009.
- Laine, S. and Aila, T. Temporal ensembling for semi-supervised learning. In *International Conference on Learning Representations*, 2017.
- Lakshminarayanan, B., Pritzel, A., and Blundell, C. Simple and scalable predictive uncertainty estimation using deep ensembles. *Advances in neural information processing systems*, 30, 2017.
- Li, J., Socher, R., and Hoi, S. C. Dividemix: Learning with noisy labels as semi-supervised learning. *arXiv preprint arXiv:2002.07394*, 2020a.
- Li, M., Soltanolkotabi, M., and Oymak, S. Gradient descent with early stopping is provably robust to label noise for overparameterized neural networks. In *International conference on artificial intelligence and statistics*, pp. 4313–4324. PMLR, 2020b.
- Liu, S., Niles-Weed, J., Razavian, N., and Fernandez-Granda, C. Early-learning regularization prevents memorization of noisy labels. *Advances in neural information processing systems*, 33:20331–20342, 2020.
- Liu, T. and Tao, D. Classification with noisy labels by importance reweighting. *IEEE Transactions on pattern analysis and machine intelligence*, 38(3):447–461, 2015.
- Lukasik, M., Bhojanapalli, S., Menon, A., and Kumar, S. Does label smoothing mitigate label noise? In *International Conference on Machine Learning*, pp. 6448–6458. PMLR, 2020.
- Ma, X., Huang, H., Wang, Y., Romano, S., Erfani, S., and Bailey, J. Normalized loss functions for deep learning with noisy labels. In *International conference on machine learning*, pp. 6543–6553. PMLR, 2020.

- Nix, D. A. and Weigend, A. S. Estimating the mean and variance of the target probability distribution. In *Proceedings of 1994 IEEE international conference on neural networks (ICNN'94)*, volume 1, pp. 55–60. IEEE, 1994.
- Patrini, G., Rozza, A., Krishna Menon, A., Nock, R., and Qu, L. Making deep neural networks robust to label noise: A loss correction approach. In *Proceedings of the IEEE conference on computer vision and pattern recognition*, pp. 1944–1952, 2017.
- Petersen, K. B., Pedersen, M. S., et al. The matrix cookbook. *Technical University of Denmark*, 7(15):510, 2008.
- Ren, M., Zeng, W., Yang, B., and Urtasun, R. Learning to reweight examples for robust deep learning. In *International conference on machine learning*, pp. 4334–4343. PMLR, 2018.
- Rusiecki, A. Standard dropout as remedy for training deep neural networks with label noise. In Zamojski, W., Mazurkiewicz, J., Sugier, J., Walkowiak, T., and Kacprzyk, J. (eds.), *Theory and Applications of Dependable Computer Systems*, pp. 534–542, Cham, 2020. Springer International Publishing. ISBN 978-3-030-48256-5.
- Sherman, J. and Morrison, W. J. Adjustment of an Inverse Matrix Corresponding to a Change in One Element of a Given Matrix. *The Annals of Mathematical Statistics*, 21(1):124 – 127, 1950. doi: 10.1214/aoms/1177729893. URL <https://doi.org/10.1214/aoms/1177729893>.
- Sukhbaatar, S., Bruna, J., Paluri, M., Bourdev, L., and Fergus, R. Training convolutional networks with noisy labels. *arXiv preprint arXiv:1406.2080*, 2014.
- Thulasidasan, S., Bhattacharya, T., Bilmes, J., Chennupati, G., and Mohd-Yusof, J. Combating label noise in deep learning using abstention. In *International Conference on Machine Learning*, pp. 6234–6243. PMLR, 2019.
- Wang, Y., Kucukelbir, A., and Blei, D. M. Robust probabilistic modeling with bayesian data reweighting. In *International Conference on Machine Learning*, pp. 3646–3655. PMLR, 2017.
- Wang, Y., Ma, X., Chen, Z., Luo, Y., Yi, J., and Bailey, J. Symmetric cross entropy for robust learning with noisy labels. In *Proceedings of the IEEE/CVF International Conference on Computer Vision*, pp. 322–330, 2019.
- Wei, J. and Liu, Y. When optimizing  $\mathcal{H}$ -divergence is robust with label noise. In *International Conference on Learning Representations*, 2021. URL <https://openreview.net/forum?id=WesiCoRVQ15>.
- Wei, J., Zhu, Z., Cheng, H., Liu, T., Niu, G., and Liu, Y. Learning with noisy labels revisited: A study using real-world human annotations. In *International Conference on Learning Representations*, 2022. URL <https://openreview.net/forum?id=TBWA6PLJZQm>.
- Xiao, T., Xia, T., Yang, Y., Huang, C., and Wang, X. Learning from massive noisy labeled data for image classification. In *Proceedings of the IEEE conference on computer vision and pattern recognition*, pp. 2691–2699, 2015.
- Xu, Y., Cao, P., Kong, Y., and Wang, Y. L<sub>dmi</sub>: A novel information-theoretic loss function for training deep nets robust to label noise. In Wallach, H., Larochelle, H., Beygelzimer, A., d’Alché-Buc, F., Fox, E., and Garnett, R. (eds.), *Advances in Neural Information Processing Systems*, volume 32. Curran Associates, Inc., 2019. URL <https://proceedings.neurips.cc/paper/2019/file/8a1ee9f2b7abe6e88d1a479ab6a42c5e-Paper.pdf>.
- Zhang, Z. and Sabuncu, M. Generalized cross entropy loss for training deep neural networks with noisy labels. *Advances in neural information processing systems*, 31, 2018.
- Zhou, X., Liu, X., Jiang, J., Gao, X., and Ji, X. Asymmetric loss functions for learning with noisy labels. In *International conference on machine learning*, pp. 12846–12856. PMLR, 2021.

## A. Derivations

### A.1. The Probability Density Function of a Logistic-Normal Distribution

Assume  $\mathbf{Y} \sim \mathcal{N}(\boldsymbol{\mu}, \boldsymbol{\Sigma})$  for some  $\boldsymbol{\mu} \in \mathbb{R}^{K-1}$ ,  $\boldsymbol{\Sigma} \in \mathbb{R}^{(K-1) \times (K-1)}$  and  $\mathbf{S} = S_C(\mathbf{Y})$ , then the probability density function (pdf) of  $\mathbf{S}$  can be written as  $f_{\mathbf{S}}(\mathbf{s}) = \text{abs}(|J(\mathbf{s})|) \cdot f_{\mathbf{Y}}(S_C^{-1}(\mathbf{s}))$ . In which,  $|J(\mathbf{s})|$ , the determinant of the Jacobian of  $S_C^{-1}(\mathbf{s}) = (\log \frac{\mathbf{s}_k}{\mathbf{s}_K})_{k \in \mathbb{N}_{K-1}}$  is given by (Dillon et al., 2017)

$$\begin{aligned}
 |J(\mathbf{s})| &= |\mathbf{D}^{-1} + \frac{\mathbf{1}}{\mathbf{s}_K}| \\
 &= |\mathbf{D}^{-1} + \frac{\mathbf{D}^{-1} \mathbf{s}_{-K} \mathbf{s}_{-K}^T \mathbf{D}^{-1}}{\mathbf{s}_K}| \\
 &= |\mathbf{D}^{-1} + \frac{\mathbf{D}^{-1} \mathbf{s}_{-K} \mathbf{s}_{-K}^T \mathbf{D}^{-1}}{1 - \mathbf{s}_{-K}^T \mathbf{D}^{-1} \mathbf{s}_{-K}}| \\
 &= (|\mathbf{D} - \mathbf{s}_{-K} \mathbf{s}_{-K}^T|)^{-1} \\
 &= (|\mathbf{D}|(1 - \mathbf{s}_{-K}^T \mathbf{D}^{-1} \mathbf{s}_{-K}))^{-1} \\
 &= \left( \prod_{k=1}^K \mathbf{s}_k \right)^{-1}
 \end{aligned} \tag{15}$$

where  $\mathbf{D} = \text{diag}(\mathbf{s}_{-K})$  and  $\mathbf{s}_{-K} = (\mathbf{s}_k)_{k \in \mathbb{N}_{K-1}}$ . The first equality is obtained by computing derivatives while  $\mathbf{s}_K = 1 - \sum_{k=1}^{K-1} \mathbf{s}_k$ , the fourth equality is based on the Sherman–Morrison identity (Sherman & Morrison, 1950) and the fifth equality holds based on the matrix determinant lemma (Harville, 1998). As  $f_{\mathbf{S}}(\mathbf{s}) = \text{abs}(|J(\mathbf{s})|) \cdot f_{\mathbf{Y}}(S_C^{-1}(\mathbf{s}))$ , the pdf of the Logistic-Normal distribution is

$$f_{\mathbf{S}}(\mathbf{s}) = \frac{1}{\prod_{k=1}^K \mathbf{s}_k} \frac{1}{|(2\pi)^{K-1} \boldsymbol{\Sigma}|^{\frac{1}{2}}} e^{-\frac{1}{2} \mathbf{r}^T \boldsymbol{\Sigma}^{-1} \mathbf{r}} = \frac{1}{\prod_{k=1}^K S_C(\mathbf{y})_k} \frac{1}{|(2\pi)^{K-1} \boldsymbol{\Sigma}|^{\frac{1}{2}}} e^{-\frac{1}{2} \mathbf{r}^T \boldsymbol{\Sigma}^{-1} \mathbf{r}} \tag{16}$$

where  $\mathbf{r} = S_C^{-1}(\mathbf{s}) - \boldsymbol{\mu} = \mathbf{y} - \boldsymbol{\mu}$ .

### A.2. Optimal Covariance Matrix

We want to show that the optimal  $\boldsymbol{\Sigma}$  matrix for example  $j$  is:  $\boldsymbol{\Sigma}_j^{opt} = (\mathbf{y}_j - \boldsymbol{\mu}_j)(\mathbf{y}_j - \boldsymbol{\mu}_j)^T = \mathbf{r}_j \mathbf{r}_j^T$ . First, we note that the gradients of the negative log likelihood in Equation 5 with respect to  $\boldsymbol{\Sigma}_j$  is:

$$\frac{\partial \mathcal{L}}{\partial \boldsymbol{\Sigma}_j} = \frac{1}{2} \sum_{i=1}^N \frac{\mathbf{r}_i^T \boldsymbol{\Sigma}_i^{-1} \mathbf{r}_i + \log |\boldsymbol{\Sigma}_i|}{\partial \boldsymbol{\Sigma}_j} = \frac{1}{2} \frac{\mathbf{r}_j^T \boldsymbol{\Sigma}_j^{-1} \mathbf{r}_j + \log |\boldsymbol{\Sigma}_j|}{\partial \boldsymbol{\Sigma}_j}$$

as all other terms of the loss are unaffected by  $\boldsymbol{\Sigma}_j$  and are therefore zero. Computing the gradients with respect to  $\boldsymbol{\Sigma}_j$  while applying two identities  $\frac{\partial}{\partial \boldsymbol{\Sigma}} \log |\boldsymbol{\Sigma}| = \boldsymbol{\Sigma}^{-1}$  and  $\frac{\partial}{\partial \boldsymbol{\Sigma}} \mathbf{r}^T \boldsymbol{\Sigma}^{-1} \mathbf{r} = -\boldsymbol{\Sigma}^{-1} \mathbf{r} \mathbf{r}^T \boldsymbol{\Sigma}^{-1}$  (see (Petersen et al., 2008) Equations 57 and 63), we have

$$\frac{\partial}{\partial \boldsymbol{\Sigma}} [\mathbf{r}_j^T \boldsymbol{\Sigma}_j^{-1} \mathbf{r}_j + \log |\boldsymbol{\Sigma}_j|] = -\boldsymbol{\Sigma}_j^{-1} \mathbf{r}_j \mathbf{r}_j^T \boldsymbol{\Sigma}_j^{-1} + \boldsymbol{\Sigma}_j^{-1} \tag{17}$$

where the latter identity being justified by properties of symmetry and trace of matrices as follows

$$\frac{\partial}{\partial \boldsymbol{\Sigma}} \mathbf{r}^T \boldsymbol{\Sigma}^{-1} \mathbf{r} = \frac{\partial}{\partial \boldsymbol{\Sigma}} \text{tr}[\mathbf{r} \mathbf{r}^T \boldsymbol{\Sigma}^{-1}] = -(\boldsymbol{\Sigma}^{-1} \mathbf{r} \mathbf{r}^T \boldsymbol{\Sigma}^{-1})^T = -\boldsymbol{\Sigma}^{-1} \mathbf{r} \mathbf{r}^T \boldsymbol{\Sigma}^{-1} \tag{18}$$

Setting the term in the right-hand side of Equation 17 to zero then left and right multiplying by  $\boldsymbol{\Sigma}_j$ , yields the maximizer of the likelihood  $\boldsymbol{\Sigma}_j^{opt} = \mathbf{r}_j \mathbf{r}_j^T$ .

### A.3. Gradients for the Mean with Optimal Covariance

The optimal covariance  $\Sigma_j^{opt} = (\mathbf{y}_j - \mu_j)(\mathbf{y}_j - \mu_j)^T = \mathbf{r}_j \mathbf{r}_j^T$  is rank 1 and is therefore not invertible. However, for an invertible  $\Sigma_j$ , we have

$$\frac{\partial \mathcal{L}}{\partial \mu_j} = -\Sigma_j^{-1} \mathbf{r}_j \Leftrightarrow \Sigma_j \frac{\partial \mathcal{L}}{\partial \mu_j} = -\Sigma_j \Sigma_j^{-1} \mathbf{r}_j = \mathbf{r}_j \quad (19)$$

This is a linear system of the form  $\mathbf{A}\mathbf{x} = \mathbf{b}$ , which can be solved with exact (or approximate) methods. If we assume  $\Sigma_j^{opt}$  is invertible (in practice this is done by adding a diagonal matrix), and solve the linear system with  $\mathbf{A} = \Sigma_j^{opt}$  instead, one solution is  $\frac{\partial \mathcal{L}}{\partial \mu_j} = \frac{\mathbf{r}_j}{\|\mathbf{r}_j\|_2^2}$  as  $\mathbf{r}_j$  is an eigenvector of  $\Sigma_j^{opt}$  with eigenvalue  $\|\mathbf{r}_j\|_2^2$ :

$$\Sigma_j^{opt} \mathbf{r}_j = (\mathbf{r}_j \mathbf{r}_j^T) \mathbf{r}_j = \mathbf{r}_j (\mathbf{r}_j^T \mathbf{r}_j) = \|\mathbf{r}_j\|_2^2 \mathbf{r}_j \quad (20)$$

**Side-note:** In practice, this is not how the gradients are computed. Typically the label-dependent part of the loss is computed with a similar rewrite as above, i.e.,  $\mathbf{r}_j \Sigma_j^{-1} \mathbf{r} = \mathbf{r}_j (\Sigma \setminus \mathbf{r})$  where  $\Sigma \setminus \mathbf{r}$  is the (exact or approximate) solution to the linear system  $\Sigma \mathbf{x} = \mathbf{r}$ , which we then do backpropagation through. This is more numerically stable than calculating the inverse and multiplying it with  $\mathbf{r}_j$ .

### A.4. The Effect of Lambda on the Optimal Variance

In this section, we provide derivations for the behavior in Figure 2. Our goal is to show how  $\lambda$  affects the optimally learned  $\sigma^2$ . First, we note that Equation 5 for binary classification becomes

$$\mathcal{L} = \frac{1}{2} \sum_{i=1}^N \frac{(y_i - \mu_i)^2}{\sigma_i^2} + \log \sigma_i^2 + C \quad (21)$$

and we want to look at  $\frac{\partial \mathcal{L}}{\partial \sigma_i^2} = 0$  for a particular example  $i$ . To simplify notation, we let  $\sigma_i^2 = \sigma^2$ ,  $y_i = y$ , and  $\mu_i = \mu$  and let  $r = y - \mu$  denote the residual. With this notation, the gradient of the loss with respect to  $\sigma^2$  for example  $i$  is

$$\frac{\partial}{\partial \sigma^2} \left[ \frac{r^2}{2\sigma^2} + \frac{1}{2} \log \sigma^2 \right] = -\frac{r^2}{2\sigma^4} + \frac{1}{2\sigma^2} = \frac{\sigma^2 - r^2}{2\sigma^4} \quad (22)$$

Solving for when the gradient is zero, gives  $\sigma_{opt}^2 = r^2$ . However, as our predicted variance is  $\sigma_\theta^2 = (c_\theta^2 + \lambda)(c_\theta^2 + \lambda) = c_\theta^4 + 2\lambda c_\theta^2 + \lambda^2$ , it cannot be smaller than  $\lambda^2$ , and therefore  $\sigma_{opt}^2$  is not always obtainable. If  $r \geq \lambda$  then  $\sigma_{opt}^2$  is obtainable with  $c_\theta^2 = r - \lambda$ . This corresponds to when the loss is one in Figure 2. However, the optimal variance is not obtainable if,  $r < \lambda$ , as it implies  $c_\theta^2 < 0$ , which is impossible. To better understand what the network does in this case, we look at the gradient of the loss with respect to  $c_\theta$

$$\frac{\partial}{\partial c_\theta} \left[ \frac{r^2}{2\sigma_\theta^2} + \frac{1}{2} \log \sigma_\theta^2 \right] = \frac{\partial}{\partial \sigma_\theta^2} \left[ \frac{r^2}{2\sigma_\theta^2} + \frac{1}{2} \log \sigma_\theta^2 \right] \frac{\partial \sigma_\theta^2}{\partial c_\theta} = \frac{(\sigma_\theta^2 - r^2)(4c_\theta^3 + 4\lambda c_\theta)}{\sigma_\theta^4} \quad (23)$$

where the first equality follows from the chain rule. Hence, in the case that  $\sigma_\theta^2 \geq \lambda^2 > r^2$ , the numerator of the gradient can only be zero if  $c_\theta$  is zero, making  $\sigma_\theta^2 = \lambda^2$ . This corresponds to the (scaled) squared error behavior for small residuals ( $r^2 < \lambda^2$ ) in Figure 2.

### A.5. Target Logits

From Section 3.2, the target categorical for  $y = i$  is:

$$S(\mathbf{y}) = ((1-t)\delta_i + t\mathbf{u})_j = \begin{cases} t/K & i \neq j \\ \frac{(1-t)K+t}{K} & i = j \end{cases} \quad (24)$$

and  $S_C^{-1}(\mathbf{p}) = \log([p_1, \dots, p_{K-1}]/p_K)$ . Hence, if  $i \neq K$ , then the observed target logit is:

$$\mathbf{y} = S_C^{-1}(S_C(\mathbf{y})) = S_C^{-1}((1-t)\delta_i + t\mathbf{u})_j = \begin{cases} 0 & i \neq j \\ \mathcal{C} & i = j \end{cases} \quad (25)$$

as  $\log(\frac{t}{K}/\frac{t}{K}) = \log 1 = 0$  and where  $\mathcal{C} = \log \frac{(1-t)K+t}{t}$ . If  $i = K$ , then we have for all  $j$ :

$$\mathbf{y} = S_C^{-1}((1-t)\delta_i + t\mathbf{u})_j = -\mathcal{C}. \quad (26)$$



### A.6. Gradients for the Heteroscedastic NN methods

In Heteroscedastic NN methods, the prediction is the mean of  $M$  samples  $\bar{\mathbf{y}}_c = \frac{1}{M} \sum_{m=1}^M \mathbf{y}_c^m$ , in which we define  $\mathbf{y}_c^m = e^{\mathbf{z}_c + \epsilon^m} / \Sigma_K^m$  and  $\Sigma_K^m = \sum_{k=1}^K e^{\mathbf{z}_k + \epsilon^m}$ . Therefore, the gradient of softmax output w.r.t logits is given by:

$$\begin{aligned}
 \frac{\partial}{\partial \mathbf{z}_j} \frac{1}{M} \sum_{m=1}^M \mathbf{y}_i^m &= \frac{1}{M} \sum_{m=1}^M \frac{\partial \mathbf{y}_i^m}{\partial \mathbf{z}_j} = \frac{1}{M} \sum_{m=1}^M \frac{\partial}{\partial \mathbf{z}_j} \frac{e^{\mathbf{z}_i + \epsilon^m}}{\Sigma_K^m} \\
 &= \frac{1}{M} \sum_{m=1}^M \frac{\delta_{ij} e^{\mathbf{z}_i + \epsilon^m} \Sigma_K^m - e^{\mathbf{z}_i + \epsilon^m} e^{\mathbf{z}_j + \epsilon^m}}{(\Sigma_K^m)^2} \\
 &= \frac{1}{M} \sum_{m=1}^M \frac{e^{\mathbf{z}_i + \epsilon^m}}{\Sigma_K^m} \left( \frac{\delta_{ij} \Sigma_K^m - e^{\mathbf{z}_j + \epsilon^m}}{\Sigma_K^m} \right) \\
 &= \frac{1}{M} \sum_{m=1}^M \mathbf{y}_i^m (\delta_{ij} - \mathbf{y}_j^m) \\
 &= \begin{cases} \frac{1}{M} \sum_{m=1}^M \mathbf{y}_i^m (1 - \mathbf{y}_j^m) & i = j \\ -\frac{1}{M} \sum_{m=1}^M \mathbf{y}_i^m \mathbf{y}_j^m & i \neq j \end{cases}
 \end{aligned}$$

Using the last equation, we can compute the derivatives of the log-likelihood with respect to logits as follows:

$$\begin{aligned}
 \frac{\partial}{\partial \mathbf{z}_j} \sum_{i=1}^K \mathbf{t}_i \log\left(\frac{1}{M} \sum_{m=1}^M \mathbf{y}_i^m\right) &= \sum_{i=1}^K \mathbf{t}_i \frac{\frac{\partial}{\partial \mathbf{z}_j} \sum_{m=1}^M \mathbf{y}_i^m}{\sum_{m=1}^M \mathbf{y}_i^m} \\
 &= \sum_{i=1}^K \mathbf{t}_i \frac{\sum_{m=1}^M \mathbf{y}_i^m (\delta_{ij} - \mathbf{y}_j^m)}{\sum_{m=1}^M \mathbf{y}_i^m} \\
 &= - \sum_{i \neq j}^K \mathbf{t}_i \frac{\sum_{m=1}^M \mathbf{y}_i^m \mathbf{y}_j^m}{\sum_{m=1}^M \mathbf{y}_i^m} \\
 &\quad + \mathbf{t}_j \left( 1 - \frac{\sum_{m=1}^M (\mathbf{y}_j^m)^2}{\sum_{m=1}^M \mathbf{y}_j^m} \right) \\
 &= \mathbf{t}_j - \sum_i^K \mathbf{t}_i \frac{\sum_{m=1}^M \mathbf{y}_i^m \mathbf{y}_j^m}{\sum_{m=1}^M \mathbf{y}_i^m}
 \end{aligned}$$

Assuming a label  $\mathbf{t} = \delta_c$  is given, we can rewrite the above equation in a simpler form:

$$\begin{aligned}
 \frac{\partial}{\partial \mathbf{z}_j} \sum_{i=1}^K \mathbf{t}_i \log\left(\frac{1}{M} \sum_{m=1}^M \mathbf{y}_i^m\right) &= \mathbf{t}_j - \sum_i^K \mathbf{t}_i \frac{\sum_{m=1}^M \mathbf{y}_i^m \mathbf{y}_j^m}{\sum_{m=1}^M \mathbf{y}_i^m} \\
 &= \mathbf{t}_j - \sum_i^K \mathbf{t}_i \frac{\sum_{m=1}^M \mathbf{y}_i^m \mathbf{y}_j^m}{\sum_{m=1}^M \mathbf{y}_i^m} \\
 &= \mathbf{t}_j - \frac{\sum_{m=1}^M \mathbf{y}_c^m \mathbf{y}_j^m}{\sum_{m=1}^M \mathbf{y}_c^m} \\
 &= \mathbf{t}_j - \sum_{m=1}^M \mathbf{y}_j^m \frac{\mathbf{y}_c^m}{\sum_{m=1}^M \mathbf{y}_c^m} \\
 &= \mathbf{t}_j - \frac{1}{M} \sum_{m=1}^M \mathbf{y}_j^m \frac{\mathbf{y}_c^m}{\frac{1}{M} \sum_{m=1}^M \mathbf{y}_c^m}
 \end{aligned}$$

The derivatives of the log-likelihood, in vector notation, are given by:

$$\begin{aligned} \frac{\partial}{\partial \mathbf{z}} \left[ \mathbf{t}^T \cdot \log \left( \frac{1}{M} \sum_{m=1}^M \mathbf{y}^m \right) \right] &= \boldsymbol{\delta}_c - \frac{1}{M} \sum_{m=1}^M \mathbf{y}^m \frac{\mathbf{y}_c^m}{\frac{1}{M} \sum_{m=1}^M \mathbf{y}_c^m} \\ &= \boldsymbol{\delta}_c - \frac{1}{M} \sum_{m=1}^M S(\mathbf{z} + \boldsymbol{\epsilon}^m) \frac{S(\mathbf{z} + \boldsymbol{\epsilon}^m)_c}{\frac{1}{M} \sum_{m=1}^M S(\mathbf{z} + \boldsymbol{\epsilon}^m)_c} \end{aligned}$$

## B. Hyperparameters

### B.1. Method-independent Hyperparameters

All methods are implemented in the same code base, using the same network architectures, optimizers, hyperparameter searches, etc. We use a learning rate of 0.0001 for synthetic datasets, 0.001 for MNIST and Clothing1M, and 0.01 for the CIFAR datasets. We show that our method performs well under different optimizers by using gradient descent for the synthetic datasets, Adam for MNIST (batch size 256), and SGD with Nesterov momentum of 0.9 for Clothing1M (batch size 32) and the CIFAR datasets (batch size 128). We use a weight decay of 1e-3 and 5e-4 for Clothing1M and the CIFAR datasets, respectively, but no such regularization for the other datasets. We use an MLP with two hidden layers with 2000 hidden units for the synthetic datasets, a convolutional network (LeNet-5) for MNIST, and residual networks for the CIFAR datasets (WideResNet-28-2) and Clothing1M (ImageNet pre-trained ResNet-50). We train for 2000, 100, 10, and 300 epochs for the synthetic datasets, MNIST, Clothing1M, and CIFAR, respectively. We use 10% of the training set of MNIST and CIFAR as a noisy validation set.

### B.2. Method-dependent Hyperparameter Search

In this section, we go over our thorough hyperparameter search we did for the results in Tables 1 and 2. For each method, we search for method-specific hyperparameters for each noise rate and noise type per dataset. For Het- $\tau$  and Het- $\tau$ - $\Sigma_{\text{full}}$ , we search for temperatures in  $[0.1, 0.5, 1.0, 10.0, 20.0]$ , while Het- $\tau$ - $\Sigma_{\text{full}}$  also searches over  $R$  of the covariance matrix in  $[1, 2, 4]$ . We choose the range of values to search over is based on the original papers. Our method searches over temperatures and  $\lambda$ s in  $[0.1, 0.5, 1.0]$  for MNIST, but  $\lambda$ s in  $[0.5, 1.0]$  for the CIFAR datasets and Clothing1M. For GCE, we search over  $q$  in  $[0.1, 0.3, 0.5, 0.7, 0.9]$ . For NAN, the search is over  $\sigma$  in  $[0.1, 0.2, 0.5, 0.75, 1.0]$ . For Bi-tempered, we search for  $t_1$  in  $[0.5, 0.7, 0.9]$  and  $t_2$  in  $[1.1, 2.0, 4.0]$ . All searches are done with a single seed, and the hyperparameters with the highest noisy validation accuracy at the end of training are used to train four more networks with different seeds. The hyperparameters used for different noise rates, noise types, and datasets are shown in Tables 4, 5, and 6.

## C. Natural Datasets

The CIFAR-10N dataset has five new sets of labels for the CIFAR-10 training set, which was generated by having each training image labeled by three different humans. Naturally, this gives rise to three different labeled sets (Random 1-3). The fourth set is generated through majority voting, where ties are broken at random (Aggregate). Finally, the last set of labels (Worst) was created by randomly picking one of the labels that are different from the original training label, if no such a label exists then the original is used. The noisy labels are 18%, 9%, and 40% of all labels for Random, Aggregate and Worst, respectively. CIFAR-100N was created similarly, but with a single human annotator per image, resulting in a noise rate of 40%. Clothing1M is a dataset of one million images of clothes from 14 different classes, automatically labeled based on captions. As there is a large imbalance between the classes, we follow the balancing strategy of Li et al. (2020a). We use the provided validation and test sets. The noise rate is estimated to be 38%.

## D. Implementation Details

We implement our method using the TensorFlow Probability (Dillon et al., 2017) library. The Logistic-Normal distribution is implemented as a transformed distribution (the TransformedDistribution class) comprised of a distribution and a transform. For the distribution, we use a multivariate normal distribution (the MultivariateNormalDiagPlusLowRank class). For the transform, we combine a softmax centered and a scale (for temperature) bijector using the Chain bijector class. Conveniently,

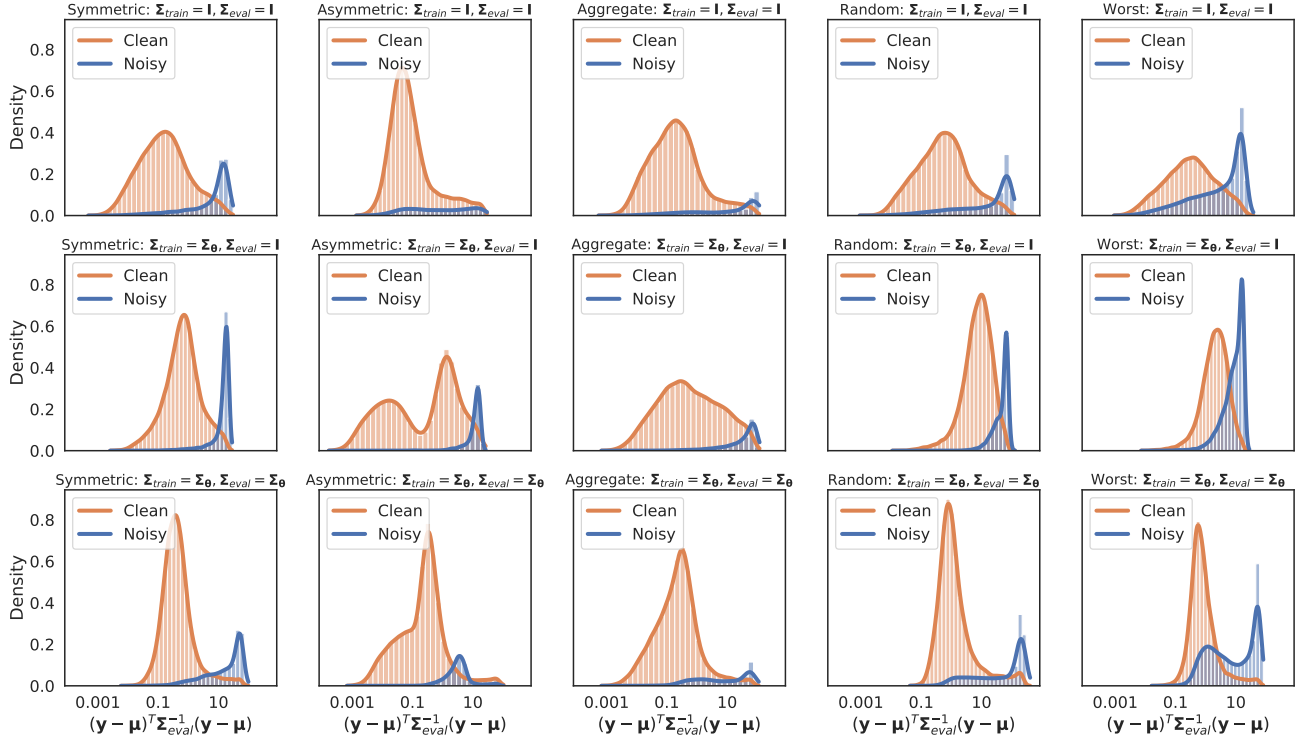


**Figure 7: Loss Attenuation: The Effect of the Covariance Matrix.** For a network trained on MNIST with 40% symmetric noise, we show the distribution of the label-dependent term of the loss with (left) and without (right) the scaling of the covariance matrix for clean and noisy examples separately. The x-axis correspond to the log-scaled loss. We find that the covariance matrix increases the loss of clean examples and reduces the loss of noisy examples.

the loss can then be implemented by using the built-in method (`log_prob`) of the transformed distribution class to calculate the logarithm of the pdf. Our code will be made publicly available upon acceptance.

## E. Additional Experiments

If not otherwise stated, all the results in the tables in this section reports the mean and standard deviation for the test accuracy over five runs with different seeds.

### E.1. Residual Histograms

In this section, we show similar histograms as in Figure 6, but for more noise types: symmetric noise and aggregate, random 2, and worst from CIFAR-10N. The setup is the same, to train two networks by minimizing the negative log-likelihood of Logistic-Normal likelihoods with different covariance matrices ( $\Sigma_{train}$ ) and evaluate the label-dependent term of Equation 5, with either  $\Sigma_{eval}$  equal to  $I$  or  $\Sigma_{\theta}$  at the end of training. See Figure 7. Comparing  $\Sigma_{train} = \Sigma_{eval} = I$  (top row) with  $\Sigma_{train} = \Sigma_{\theta}, \Sigma_{eval} = I$  (middle row) that the former reduces the residuals of more of the noisy examples than the latter, which indices learning  $\Sigma$  is more robust. Furthermore, comparing  $\Sigma_{train} = \Sigma_{\theta}, \Sigma_{eval} = I$  (middle row) with  $\Sigma_{train} = \Sigma_{\theta}, \Sigma_{eval} = \Sigma_{\theta}$  (bottom row), we find that  $\Sigma_{\theta}$  increases the loss for some clean examples and reduces the loss of high-residual examples, both clean and noisy ones.

Table 4: **Hyperparameters used for Synthetic (symmetric) Noise on MNIST and CIFAR datasets.** A hyperparameter search over method-specific hyperparameters is done, and the best values are shown here. For Het- $\tau$ , we report the temperature, for Het- $\tau$ - $\Sigma_{\text{full}}$  the temperature and the number of factors ( $R$ ), for GCE  $q$ , for Bi-tempered  $t_1$  and  $t_2$ , for NAN  $\sigma$ , and for LN the temperature and  $\lambda$ .

Dataset	Method	No Noise	Symmetric Noise Rate				
		0%	20%	40%	60%	80%	
MNIST	Het- $\tau$	0.5	0.1	20	10	20	
	Het- $\tau$ - $\Sigma_{\text{full}}$	[1.0, 1]	[0.1, 4]	[0.1, 4]	[10, 4]	[0.1, 1]	
	Bi-tempered	[0.9, 1.1]	[0.7, 4.0]	[0.5, 4.0]	[0.5, 4.0]	[0.7, 4.0]	
	NAN	0.2	1.0	1.0	1.0	1.0	
	GCE	0.3	0.7	0.9	0.9	0.9	
	LN	[1.0, 1.0]	[1.0, 1.0]	[1.0, 0.5]	[0.5, 0.1]	[1.0, 0.1]	
CIFAR-10	Het- $\tau$	0.5	10	20	10	10	
	Het- $\tau$ - $\Sigma_{\text{full}}$	[0.5, 4]	[20, 4]	[20, 1]	[10, 2]	[10, 4]	
	Bi-tempered	[0.9, 2.0]	[0.5, 2.0]	[0.7, 2.0]	[0.9, 2.0]	[0.7, 2.0]	
	NAN	0.2	0.5	0.75	0.75	0.75	
	GCE	0.1	0.9	0.9	0.9	0.9	
	LN	[0.1, 0.5]	[0.5, 0.5]	[1.0, 0.5]	[1.0, 0.5]	[1.0, 0.5]	
CIFAR-100	Het- $\tau$	20	20	10	10	0.1	
	Het- $\tau$ - $\Sigma_{\text{full}}$	[0.5, 4]	[10, 4]	[10, 4]	[10, 1]	[1, 1]	
	Bi-tempered	[0.7, 1.1]	[0.5, 1.1]	[0.5, 1.1]	[0.7, 1.1]	[0.7, 1.1]	
	NAN	0.1	0.2	0.2	0.2	0.2	
	GCE	0.5	0.5	0.5	0.5	0.3	
	LN	[0.1, 0.5]	[1.0, 0.5]	[1.0, 0.5]	[1.0, 0.5]	[1.0, 0.5]	

Table 5: **Hyperparameters used for Synthetic (asymmetric) Noise on MNIST and CIFAR-10.** A hyperparameter search over method-specific hyperparameters is done, and the best values are shown here. For Het- $\tau$ , we report the temperature, for Het- $\tau$ - $\Sigma_{\text{full}}$  the temperature and the number of factors ( $R$ ), for GCE  $q$ , for Bi-tempered  $t_1$  and  $t_2$ , for NAN  $\sigma$ , and for LN the temperature and  $\lambda$ .

Dataset	Method	Asymmetric Noise Rate			
		10%	20%	30%	40%
MNIST	Het- $\tau$	0.5	0.5	0.5	0.1
	Het- $\tau$ - $\Sigma_{\text{full}}$	[0.5, 2]	[10, 2]	[0.5, 1]	[10, 1]
	Bi-tempered	[0.7, 2.0]	[0.7, 4.0]	[0.5, 4.0]	[0.5, 4.0]
	NAN	0.75	1.0	0.75	1.0
	GCE	0.7	0.7	0.5	0.3
	LN	[1.0, 0.1]	[0.5, 0.1]	[0.5, 0.1]	[0.5, 0.1]
CIFAR-10	Het- $\tau$	0.5	10	10	20
	Het- $\tau$ - $\Sigma_{\text{full}}$	[0.1, 2]	[20, 2]	[0.1, 2]	[0.5, 2]
	Bi-tempered	[0.7, 1.1]	[0.7, 1.1]	[0.9, 2.0]	[0.5, 1.1]
	NAN	0.2	0.5	0.1	0.2
	GCE	0.9	0.9	0.9	0.1
	LN	[0.5, 0.5]	[0.5, 0.5]	[0.5, 0.5]	[0.5, 0.5]
CIFAR-100	Het- $\tau$	20	20	20	10
	Het- $\tau$ - $\Sigma_{\text{full}}$	[20, 2]	[20, 2]	[20, 1]	[20, 1]
	Bi-tempered	[0.5, 1.1]	[0.5, 1.1]	[0.5, 1.1]	[0.5, 1.1]
	NAN	0.2	0.1	0.2	0.1
	GCE	0.5	0.7	0.7	0.5
	LN	[1.0, 0.5]	[0.5, 0.5]	[0.5, 1.0]	[0.5, 1.0]



**Table 6: Hyperparameters used for Natural Noise** A hyperparameter search over method-specific hyperparameters is done, and the best values are shown here. For Het- $\tau$ , we report the temperature, for Het- $\tau$ - $\Sigma_{\text{full}}$  the temperature and the number of factors ( $R$ ), for GCE  $q$ , for Bi-tempered  $t_1$  and  $t_2$ , for NAN  $\sigma$ , and for LN the temperature and  $\lambda$ .

Method	CIFAR-10N					CIFAR-100N	Clothing1M
	Random 1	Random 2	Random 3	Aggregate	Worst		
Het- $\tau$	10	20	20	0.5	20	20	0.1
Het- $\tau$ - $\Sigma_{\text{full}}$	[10, 4]	[0.1, 1]	[20, 1]	[20, 1]	[10, 4]	[10, 1]	[0.1, 1]
Bi-tempered	[0.5, 2.0]	[0.5, 2.0]	[0.9, 2.0]	[0.7, 2.0]	[0.5, 2.0]	[0.5, 1.1]	[0.5, 2.0]
NAN	0.75	0.5	0.5	0.5	0.75	0.2	0.2
GCE	0.9	0.7	0.9	0.5	0.9	0.5	0.9
LN	[0.5, 0.5]	[1.0, 0.5]	[0.5, 0.5]	[1.0, 1.0]	[0.5, 0.5]	[0.5, 0.5]	[1.0, 1.0]